



HAL
open science

MIR spectral characterization of plastic to enable discrimination in an industrial recycling context: II. Specific case of polyolefins

Charles Signoret, Anne-Sophie Caro-Bretelle, José-Marie Lopez-Cuesta, Patrick Ienny, Didier Perrin

► **To cite this version:**

Charles Signoret, Anne-Sophie Caro-Bretelle, José-Marie Lopez-Cuesta, Patrick Ienny, Didier Perrin. MIR spectral characterization of plastic to enable discrimination in an industrial recycling context: II. Specific case of polyolefins. *Waste Management*, 2019, 98, pp.160-172. 10.1016/j.wasman.2019.08.010 . hal-02424758

HAL Id: hal-02424758

<https://imt-mines-ales.hal.science/hal-02424758v1>

Submitted on 6 Jan 2020

HAL is a multi-disciplinary open access archive for the deposit and dissemination of scientific research documents, whether they are published or not. The documents may come from teaching and research institutions in France or abroad, or from public or private research centers.

L'archive ouverte pluridisciplinaire **HAL**, est destinée au dépôt et à la diffusion de documents scientifiques de niveau recherche, publiés ou non, émanant des établissements d'enseignement et de recherche français ou étrangers, des laboratoires publics ou privés.

MIR spectral characterization of plastic to enable discrimination in an industrial recycling context: II. Specific case of polyolefins

Charles Signoret, Anne-Sophie Caro-Bretelle, José-Marie Lopez-Cuesta, Patrick Ienny, Didier Perrin *

C2MA, IMT Mines Ales, Univ Montpellier, 7 Avenue Jules Renard 30100 Ales, France

ABSTRACT

Sorting at industrial scale is required to perform mechanical recycling of plastics in order to obtain properties that could be competitive with virgin polymers. As a matter of fact, the most part of the various types of plastic waste are not miscible and even compatible. Mid-Infrared (MIR) HyperSpectral Imagery (HSI) is viewed as one of the solutions to the problem of black plastic sorting. Many Waste of Electrical and Electronic Equipment (WEEE) plastics are black. Nowadays, these materials are difficult to sort at an industrial scale because the main used pigment to produce this color, carbon black, masks the Near-Infrared (NIR) spectra of polymers, the currently most used technology for acute sorting in industrial conditions.

In this study, laboratory Fourier-Transform Infrared (FTIR) in Attenuated Total Reflection mode (ATR) has been used as a theoretical toolbox based on physical chemistry to help building an automated HSI discrimination despite its limited conditions, especially shorter wavelengths ranges. Weaker resolution and very short acquisition times are other HSI limitations. Helping fast and exhaustive laboratory characterizations of polymeric waste stocks is the other goal of this study. This study focusses on polyolefins as they represent the second biggest fraction of WEEE plastics (WEEP) after styrenics and since little quantities mixed to styrenics during mechanical recycling can lead to important decrease in mechanical properties. Twelve references were thus evaluated and compared between each other and with real waste samples to highlight spectral elements, which can enable differentiation. Charts compiling the signals of discussed polymers were built aiming to the same objective.

Keywords:

Polymer recycling
Sorting
MIR
WEEE
Identification
Polyolefins

Abbreviations: **ABS**, Acrylonitrile Butadiene Styrene; **ATR**, Attenuated Total Reflection; **CaCO₃**, calcium carbonate or calcite (chalk); **DSC**, Differential Scanning Calorimetry; **ELV**, End-of-Life Vehicles; **EPDM**, Ethylene Propylene Diene Monomer; **EPR**, Ethylene Propylene Rubber; **EVA**, Ethylene Vinyl Acetate; **EOI**, End-of-Life; **FTIR**, Fourier Transform Infrared; **HDPE**, High Density Polyethylene; **HIPS**, High Impact Polystyrene; **HSI**, Hyperspectral Imagery; **LIBS** or **LIPS**, Laser Induced Breakdown/Plasma Spectroscopy; **LDPE**, Low Density Polyethylene; **LWIR**, Long Wavelength Infrared (7.4–14.0 μm or 1350–700 cm^{-1}); **MIR**, Mid-Infrared (4000–400 cm^{-1} or 2.5–25.0 μm); **MWIR**, Middle Wavelength Infrared – 2 to 5 μm (5000 to 2000 cm^{-1}); **PC**, Polycarbonate (from bisphenol A); **PE**, Polyethylene (HDPE or LDPE); **PEG**, Polyethylene glycol (=POE); **PET**, Polyethylene terephthalate; **PEX**, Cross-linked (X) Polyethylene; **POE**, Polyoxyethylene (=PEG); **POM**, Polyoxyethylene; **PMMA**, Polymethylmethacrylate; **PP**, Polypropylene; **PPC** or **PP copo**, Polypropylene copolymer; **PPH** or **PP homo**, Polypropylene homopolymer; **PPE** or **PPO**, Polyphenylene ether or Polyphenylene oxide; **PVC**, Polyvinyl chloride; **PS**, Polystyrene; **THz**, Terahertz; **WEEE** or **W3E**, Waste of Electrical & Electronic Equipment; **XLPE**, Cross-linked LDPE; **XRF**, X Rays Fluorescence; **XRT**, X Rays Transmission.

* Corresponding author.

E-mail address: didier.perrin@mines-ales.fr (D. Perrin).

1. Introduction

Plastic waste pollution is getting more and more attention, firstly because of the more and more mediatized “Great Pacific Garbage Patch” (Koelmans et al., 2015; Lebreton et al., 2018), also called “7th continent”. Recently, Matiddi et al. (2017) found that 85% of Mediterranean loggerhead sea turtles found dead on the Italian Coast, had ingested plastic. On another scale, microplastics are also gaining awareness as several studies found them everywhere in consumable water and along the food chain (Gallo et al., 2018; Huerta Lwanga et al., 2017; Li et al., 2016). It is however very difficult to evaluate potential effects on human health and, more generally, on the global ecosystem (Thompson et al., 2009). Additionally, potentially toxic additives lead to increasing concerns (Dimitrakakis et al., 2009; Gallo et al., 2018), especially bisphenol A (BPA) (Le Magueresse-Battistoni et al., 2018; Rahmani et al., 2018), phthalates (Muñoz et al., 2018; Pivnenko et al., 2016) and brominated flame retardants (Aldrian et al., 2015; Gallen et al., 2014), as they could migrate from their

matrices and have harmful effects on humans. Finally, the very synthesis of plastics is denounced as the large majority is issued from fossil resources (“The new plastics economy: Rethinking the future of plastics” 2016).

Mechanical recycling, the re-processing of materials, generally by melting, is generally described as one of the most cost-efficient and eco-friendly ways to revalorize End-of-Life (EoL) products (Cosate de Andrade et al., 2016; Gundupalli et al., 2017; WRAP, 2008). However, it meets several strong limitations, as management and collection are complex. This is partially explained by differences of regional policies, education and infrastructures (Cucchiella et al., 2015; Steg and Vlek, 2009; Xanthos and Walker, 2017). In the specific case of polymers, ageing during service life, mainly by photo and/or thermo-oxidation, and reprocessing often leads to property decreases (Celina, 2013). Another obstacle is the strong incompatibility between most polymers which makes industrial sorting mandatory to obtain satisfying properties (Perrin et al., 2016). The two main industrial plastic sorting technologies are densimetric separation (sink-float) (Pongstabodee et al., 2008) and NIR-HSI (Near-InfraRed Hyperspectral Imagery) (Beigbeder et al., 2013; Serranti et al., 2011). However, they are limited, respectively by overlapping densities and large use of carbon black as a colorant, especially in Waste of Electrical and Electronic Equipment (WEEE) and plastics from End of Life Vehicles (ELV). Styrenics will tend to overlap more and more because of the increasing use of blends (mainly ABS-PC, ABS-PMMA, HIPS-PPE) (Peeters et al., 2015). Unloaded polyolefins are generally retrieved thanks to water sink-float separation. Indeed, they are the only polymers with intrinsic densities (excluding foams) below 1 g/cm^3 (Gent et al., 2009). A non-negligible fraction is found at higher densities because of heavy loadings of CaCO_3 , or talc (Maris et al., 2015). Flame retardants can also have the same effect of overlapping densities (Peeters et al., 2014).

Maris et al. (2015) found 29% ABS, 26% HIPS, 5% ABS/PC (thus 60% styrenics) and 22% PP within their batches of WEEE plastics. Dimitrakakis et al. (2009) found 37% ABS, 19% PS (supposedly HIPS) and 29% PP. Finally, Stenvall et al. (2013) found 38% ABS, 42% HIPS and 10% PP. Nevertheless, styrenics, the main fraction of WEEE plastics (WEEP), cannot accept polyolefins during reprocessing, because even a few percent can lead to very important decreases of impact resistance (Perrin et al., 2016). When dealing with these waste stocks, it is thus important to discriminate styrenics and polyolefins. Moreover, new technologies capable of sorting black plastics could aim to compete with NIR-HSI on other waste stocks, as in municipal waste where polyolefins are far more present, making their identification and distinction essential. Especially, PE, which is reported as very unusual in WEEP (Dimitrakakis et al., 2009; Maris et al., 2015; Stenvall et al., 2013) is much more present in municipal waste (Lingaiah et al., 2001). Also, Eriksen and Astrup found that 10–11% of their source-separated rigid plastics from Copenhagen were black (Eriksen and Astrup, 2019).

We reported in our previous work (Signoret et al., 2019) that LIBS and Raman are two of the preferred alternatives in the scientific literature. In general, spectroscopic/optic technologies are considered as the most precise ones for polymer sorting (Gundupalli et al., 2017). Küter et al. (2018) recently worked on Terahertz (THz) imaging applied to black plastics sorting, from camera conception to sorting line design, and include classification algorithms. They proved that this very recent technology was adapted to distinguish pristine plastic sheets of ABS and PP. A very different strategy, gaining more and more attention, involves pre-treatments of polymers to perform froth flotation (Thanh Truc et al., 2017; Wang et al., 2015). Even if some results were encouraging, industrial feasibility was not achieved. In addition, polymer ageing could disrupt these treatments. Finally, surface functional-

ization could affect recycled material properties, especially by reacting during extrusion.

MIR ($4000\text{--}400\text{ cm}^{-1}$, $2.5\text{--}25.0\text{ }\mu\text{m}$) was chosen in this study because of HSI cameras availability and the capability of FTIR (Fourier Transform Infrared) laboratory spectrometers to precisely identify polymers. However, HSI cameras operating in MIR do not currently cover the full range but only MWIR, Middle Wavelength Infrared ($2\text{--}5\text{ }\mu\text{m}$, $5000\text{--}2000\text{ cm}^{-1}$), or LWIR, Long Wavelength Infrared ($7.4\text{--}14.0\text{ }\mu\text{m}$, $1350\text{--}700\text{ cm}^{-1}$), even if the limits given here are subjects to variations. Scientific literature about extending MWIR photosensors limits, not necessary about HSI application, is pretty rich nowadays (Delmas et al., 2017; Serincan et al., 2018; Ueno et al., 2015), demonstrating that these limits could change in the future. A few papers also focused on its application to plastics identification. Becker et al. (2017) studied the application of an internally developed converter that could transform MIR (Mid-Infrared) signals into NIR, analyzable with well-developed NIR-HSI cameras. However, the relevant wavelengths range is already reachable with current commercial MIR-HSI cameras. Also, they showed measures on virgin references only. Rozenstein et al. (2017) used reflectometers which worker in a MWIR range they defined as $3\text{--}12\text{ }\mu\text{m}$. However, measures were made at the scale of a second, thus closer to static FT-IR than to industrial HSI where the total analysis time is more about several tens milliseconds (Beigbeder et al., 2013). Presented technology could conversely be useful for manual sorting. Kassouf et al. (2014) applied Independent Components Analysis to FTIR-ATR to permit plastics discrimination but only considered virgin packaging samples.

Articles cited just above mainly focused on technological and computational matters. Thus, this present study aims to evaluate MIR theoretical potential from a more physicochemical point of view with discussion on a more detailed range of polymers (e.g. PPH/PPC instead of just PP). As styrenics, main polymers among WEEP, were already considered in a previous work (Signoret et al., 2019), this present article focus on polyolefins, The objective here is to differentiate from each other and from styrenics.

PVC and POM were also considered because of their chemical structure, leading to spectral likeness with polyolefins. Through peaks wavenumbers rather exhaustive compilation, this study aims to provide a theoretical toolbox for the conception of industrial discrimination of dark plastics through MIR-HSI, especially as a potential base for the development of supervised classification algorithms. The second objective is to perform a fast and most precise laboratory characterization of polymeric waste stocks, with consideration of many materials and most of their signals.

2. Materials and methods

2.1. Materials

The types of standard samples considered were selected from bibliographic researches but also from analysis of real waste samples provided by Suez Company (France), especially from WEEP and municipal deposits. This study is focused on polyolefins encountered in WEEE streams, principally PP (polypropylene), homopolymer (PPH) and copolymer (PPC), and PE (polyethylene), mainly HDPE rather than LDPE (respectively high and low density). Also, copolymers involving ethylene and/or polypropylene were included: EPDM (ethylene-propylene-diene monomer) and EVA (ethylene-vinyl acetate). PVC is also very present in municipal deposits and POM is also found in WEEE, included in this study because of their spectral likeness. As POM is found copolymerized with ethylene glycol but no copolymer standard was available, a PEG reference was also incorporated. A comparison to styrenics, HIPS and ABS, was also done. Virgin plastic references used in

pellets to produce standard samples are presented in Table 1, with the exception of PVC and PEG directly analyzed in powder form:

Some samples from a collection of commercial materials, from the “Materiautech” of Allizé-Plasturgie (Allizé-Plasturgie, n.d.), were analyzed for complementary information, when pellets were unavailable or to check potential composition ratios variations for blends and/or copolymers (Table 2):

112 waste samples were kindly provided by the Suez Company from their plants in Feyzin (SUEZ RV DEEE) and Berville-sur-Seine (NORVAL) in France. 14 were identified as PP, 4 as PE, 1 as PEX, 2 as EVA, 11 as PVC and 3 as POM thanks to visual comparisons of their FTIR-ATR spectra to those of virgin samples and/or thanks to the most significant peaks patterns tracking as described in this study, but on the whole MIR range. Their spectra are given in supporting information. Some of them are also presented in Results & Discussion to corroborate standard results. Other samples were mainly styrenics (HIPS, ABS) and styrenics blends (HIPS/PPE, ABS/PC...). They were considered in another work (Signoret et al., 2019). A calcite sample of Omya BL (Omya) and a talc sample of Luzenac HAR T84 (IMERYS) were also analyzed.

2.2. Micro-Injection

Small disks, with a diameter of 25 mm and a thickness of 1.5 mm, were injected to serve as virgin standard samples. They were produced thanks to a Zamak-Mercator injection molding machine. Closer to small-scale transfer molding, this equipment allows to work on a few grams of pellets. This shape was chosen for reproducibility of ATR spectra as every disk has a similar surface aspect, flat and smooth enough for good detection. All references described in Table 1, with exception of PVC and PEG, were injected to produce standard samples.

2.3. FTIR-ATR Spectroscopy

A Vertex 70 FT MIR spectrometer from Bruker with an ATR unit was used. The used resolution was of 4 cm^{-1} , 16 scans for background acquisition and 16 scans for the sample spectrum. Spectra were acquired from 4000 to 400 cm^{-1} and analyzed thanks to the OPUS software provided with the spectrometer. Most of samples were directly analyzed on the crystal. Some of them needed to be cut to get a smooth enough surface for a good acquisition of the spectrum. Samples were cleaned with ethanol. FTIR-ATR (Attenuated Total Reflection) was chosen for convenience and to be closer to HSI cameras as they both work reflectively. However, ATR works with direct contact to the sample whereas HSI is remote. ATR is very sensible to contact quality and thus surface

Table 1
List of polymer pellets references.

Polymer	LDPE	HDPE	EPDM	PPH	PPC	PPC
Commercial name	2100NT00	ALCUDIA 4810	NORDEL IP 3745P	505P	PHC27	48 M10
Supplier	LG Chem	Repsol	Dow Chemical	Sabic	Sabic	Sabic
Polymer	EVA	PVC	PEG 100,000	HIPS		ABS
Commercial name	Alcudia® PA-440	EH 617-7438	18,198-6	Polystyrol 495F		Terluran GP-22
Supplier	Repsol	Benvic	Sigma-Aldrich	BASF		BASF

Table 2
List of used “Materiautech” references.

Polymer	EPDM	LDPE	PVC	POM
Reference	I/140	I/401	TF/2	I/171
Commercial name	FORPRENE 6SD001A	FE 8000	-	Keptal F40-03
Supplier	Softer	Total	Polidou	Korea Engineering Plastics Co.

quality. Roughness, pollution or non-flat surfaces are very detrimental to ATR signal-to-noise ratios. These sensibilities are likely not shared by HSI, or at least differently.

2.4. Description of the methodology for spectra comparison

The overall methodology is based on the use of charts as Table 3 which makes the inventory of every encountered significant signal within considered ranges, classifying them thanks to their wavenumbers, within 10 cm^{-1} wide columns, meaning that specified signals are 10 cm^{-1} around at max. This width was chosen in anticipation of degraded resolution of industrial apparatus. One could easily merge columns if resolutions are proven worse. Other charts are available in supporting information (for size reasons), covering both MWIR and LWIR, and both polyolefins and styrenics. The applied colors hint the relative intensities of the corresponding signal within the considered range, from pale yellow for hardly discernible signals to purple for outstanding intense peaks. These charts highlight very characteristic signals and then guide identification and discrimination, which were then taken further through direct spectra visual comparisons. This methodology was applied to identify waste samples and to develop discussion below. These charts can also serve as a solid base for supervised classification algorithms.

The MWIR ($5000\text{--}2000\text{ cm}^{-1}$) charts were limited between 3080 cm^{-1} and 2240 cm^{-1} as no significant signals were seen elsewhere for the considered polymers. The LWIR chart in supporting information was intentionally built with a wider range than commercial ones ($\approx 1350\text{--}700\text{ cm}^{-1}$) to integrate interesting signals just below (C–Cl stretching at $600\text{--}700$) and just above (CH_2 and CH_3 bending about 1400 and moreover the C=O stretching from 1550 to 1800 depending on its chemical environment). When comparing data from charts and virgin samples to real waste samples, peaks positions were found to be reproducible from a sample to another. Mentions of MWIR and LWIR throughout the text refer to these extended wavenumber ranges, but do not include other technological considerations as limited resolution.

3. Results and discussion

3.1. General features of polyolefins

Polyolefins are rather simple in their chemical natures, consisting almost exclusively of carbon and hydrogen linked by simple covalent bonds, explaining the small number of signals in MIR (Fig. 1), displaying of the simplest spectra of organic compounds. Especially, PE mainly contains CH_2 groups. PP also contains CH_3 ,

Table 3
Extract of LWIR polyolefins specific signals – color hints relative intensity.

	Polymer	1375	1365	1240	1170	1090	1015	995	975	960	840	730	720	700	630	610
PE based	PEX		1367			1090						730	719			
	EVA		1370	1236			1019						720			
	LD&HDPE											730	719			
	EPDM	1377											720			
PP based	PP homo	1375	1360		1167			997	973		841					
	PP copo	1375	1360		1167			997	973		841		720			
Others	PVC			1242		1095				963				698	630	610
	POM	1383		1236		1089	1000-700 peaks at 890 & 925							629		

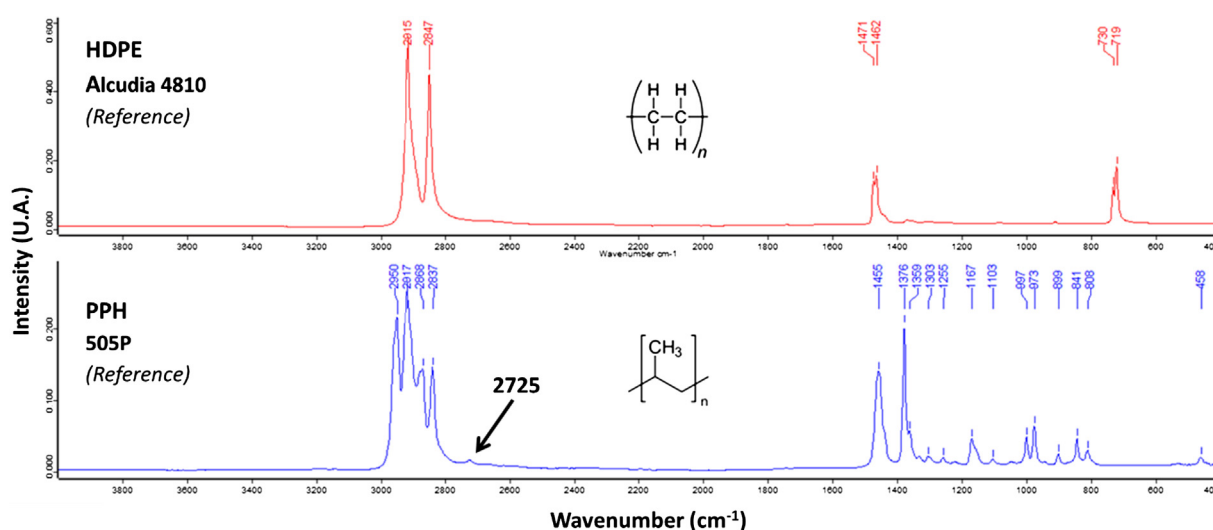


Fig. 1. Differences between HDPE and PP homopolymer reference samples in MIR – characteristic PP signal arrowed.

allowing more vibrations combinations which induce four strong signals ($2950, 2917, 2868$ & 2837 cm^{-1}) instead of just two for PE (2915 & 2847 cm^{-1}) in MWIR. The MWIR chart in [supporting information](#) highlights that they only have the $2915\text{--}2917\text{ cm}^{-1}$ in common. The 2847 cm^{-1} is characteristic of PE. Moreover, PP displays a very weak but very specific signal at 2725 cm^{-1} , seen on all waste samples and “alone” in its column within the MWIR chart. [Rabello and White \(1997\)](#) chose it as “the most appropriate” reference peak that enabled “reproducible determinations”. More than the numbers of peaks, the spread of observed signals and gaps between them could help differentiation with degraded resolution, as PP spread on more than 110 cm^{-1} with 30 or 50 cm^{-1} wide gaps whereas PE displays a unique 70 cm^{-1} wide gap. In LWIR, the peaks at $720\text{--}730\text{ cm}^{-1}$ are seen in PE, as they are associated with chained CH_2 ([Noda et al., 2007](#)), but not in PP homopolymer where each CH_2 is isolated. The 1375 cm^{-1} peak is famously associated to CH_3 in-the-plane bending, thus very strong in PP, and very weak in PE where it only corresponds to chain and ramifications ends. Several medium signals are also found between 800 and 1170 cm^{-1} for PP, corresponding to different C–H rocking below 1000 and C–C stretching above ([Noda et al., 2007](#)). Discrimination should be successful as PE only displays one specific signal, however close to the low boundary of LWIR (and even out of scope for several commercial cameras) and thus maybe subject to baseline or sensibility disturbances. PP instead shows several signals, however rather weak, which could be a concern at low sensitivity.

In summary, PE is characterized by a lack of signals in both MWIR and LWIR. PP possesses more, but mainly on same ranges as both materials exclusively contains C–H and C–C bonds, impurities, additives and ageing put aside.

3.2. Ethylene-based polymers: LDPE, HDPE, PEX and EVA

3.2.1. LDPE & HDPE: Low and high density PolyEthylene

LDPE being more easily processed and flexible, and HDPE having higher mechanical properties in general, it could be industrially interesting to separate them during recycling. [da Silva and Wiebeck \(2017\)](#) showed that it was possible to discriminate LDPE, HDPE and their blends through FTIR-ATR or Raman thanks to modified algorithms. Although, they highlighted that the spectral differences are very subtle, and that additives can bring stronger features than intrinsic HDPE/LDPE differences, which severely hinders discrimination within a complex waste stock where several polymer grades, with potentially different formulations, are mixed. The main differences between HDPE and LDPE are linked to branching and chain length, thus LDPE (linear LDPE) is an intermediate case. These differences are visible through CH_3 typical vibrations, especially at 2950 cm^{-1} and 1375 cm^{-1} framed in red on [Fig. 2](#). The first one is just seen as a subtle shoulder and the second one culminates at 1367 in HDPE but at 1376 in LDPE ([Gulmine et al., 2002](#)). [Jung et al. \(2018\)](#) also recommended LDPE/HDPE discrimination thanks to this shoulder. For intermediate cases, they

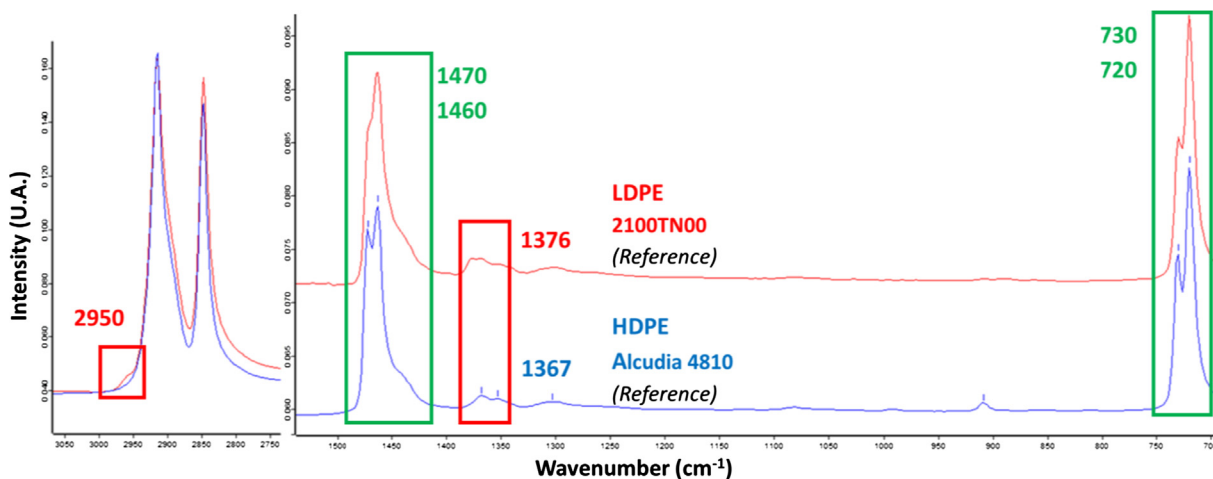


Fig. 2. LDPE and HDPE reference samples in MIR – red frames for CH₃ peaks & green frames for crystallinity markers. (For interpretation of the references to color in this figure legend, the reader is referred to the web version of this article.)

recommend measuring density. However, formulation can heavily distort density. Whereas municipal waste contains significant quantities of unformulated polyolefins (transparency/translucency/absence of color are a good hint), furniture, ELV or WEEP rarely comply with this condition. Crystallinity is another indication as LDPE is generally less crystalline than HDPE. The 720 + 730 cm⁻¹ peaks for chaining CH₂ out-of-plane bending are the most visible example, the duality of peaks induced by the duality of phases. The peaks at 1460 + 1470 cm⁻¹ for CH₂ in-plane bending are the other marker. These couples, framed in green on Fig. 2, are less distinct in LDPE than in HDPE, as proved by Hagemann et al (Hagemann et al., 1989). Also, the ratios of 720 on 730 cm⁻¹ and 1460 on 1470 cm⁻¹ are stronger with low crystallinity (Hagemann et al., 1989; Noda et al., 2007).

Finally, main differences between HDPE and LDPE relies on CH₃ presence, shown through a shoulder at 2950 cm⁻¹ (MWIR) and a stronger 1376 cm⁻¹ peak (LWIR limit), and crystallinity differences, shown through peaks duality at 1470 + 1460 and 730 + 720 cm⁻¹ (LWIR). However, these considerations are probably too subtle for industrial measurements, as intensity differences are very small and concerned wavenumbers very close, explaining why they were not differentiated in the MWIR & LWIR charts. Also, crystallinity is conditioned by thermal history, degradation level and formulation. Even at laboratory scale, this duality should be considered as hints or confirmation elements but not formal proof. Thus, real waste samples of this study were classified as “PE”: “rather LD” or “rather HD” without settling one way or the other, as differences were not conclusive enough. Even finer discriminations among HDPE/LDPE/LLDPE/MDPE/UHMWPE should rely on other laboratory technologies as DSC or GPC.

3.2.2. PEX: Crosslinked PE

One PEX sample was found within the waste stock, in the form of a blue water pipe. PEX stands for crosslinked PE. It is obtained thanks to peroxide, silane or electron beam treatments (Kelley et al., 2014). It is more and more used in plumbing (Kelley et al., 2014) as it is cheaper, does not feature corrosion issues in comparison to its metallic equivalents and can display a whole better environmental performance than more classic options (Asadi et al., 2016). However, PEX is a concern in mechanical recycling since it has poorer processability as a thermoset (Baek et al., 2016; Shamsaei et al., 2017) and represents an infusible fraction when mixed to regular PE. Sadly, they have very similar spectra, even identical in MWIR (Fig. 3). The main spectral differences are asso-

ciated with oxidation, which can also be due to polymer ageing. However, the PEX (red curve) C—O stretching at 1090 is sharper than in the sample n°1.26 of aged PE (green curve), which could be explained by the fact that crosslinking is a targeted process while ageing is not. These signals can also be linked to the presence of oxygen containing additives or fillers, as talc in the example in Fig. 3. Oliveira and Costa (2010) got slightly different oxidation marks for their silane crosslinked HDPE but signals were still rather weak, hardly seen, even in FTIR-ATR. In Fig. 3, the PEX sample displays crystallinity signals that are intermediate between HDPE and LDPE of Fig. 2. PEX is generally synthesized from HDPE, but can also be made from LDPE, rather called “XLPE” then (Oliveira and Costa, 2010). Also, cross-linking diminishes crystallinity as chains are restrained.

PEX is different from PE through oxidation marks in LWIR around 1090 cm⁻¹, but in a slight measure, probably less intense than what could be due to ageing or filling. Other PEX references, sadly unavailable here, should analyzed to consolidate these conclusions but no important differences are to be expected since crosslinking of PE concerns only a few macromolecular chains. Thus, it can be expected that spectral differences between HDPE, LDPE and PEX are too weak to be distinguished with low spectral resolution and sensitivity. Ageing, presence of additives and fillers worsen the issue. For laboratory analysis of these three materials, one should rely on complementary techniques as DSC (Differential Scanning Calorimetry). As PEX main application is plumbing, specific collection schemes could be performed to avoid mixing it to other polyolefins. Elemental technologies, as LIBS, XRT (X rays transmission) or XRF (X rays fluorescence) could be interesting for silane crosslinked PE, even if silicon concentrations could be too low for discrimination.

3.2.3. EVA: Ethylene vinyl acetate

EVA is a copolymer of ethylene and vinyl acetate with a very low melting point whose very polar groups permit pseudo-elastomeric properties. Within the studied waste stock, it was mainly found in vacuum cleaner hoses as they need to be flexible. As an impurity during recycling, it could bring ductility and impact strength if compatibility is sufficient. However, negative impacts on modulus and maximum strength are to be expected. It is identical to PE (and thus PEX) in MWIR but different in LWIR, especially with the C—O stretching signals at 1235 and 1020 cm⁻¹ (Noda et al., 2007) framed in blue on Fig. 4 and very specific as they belong to empty columns of the LWIR chart in supporting

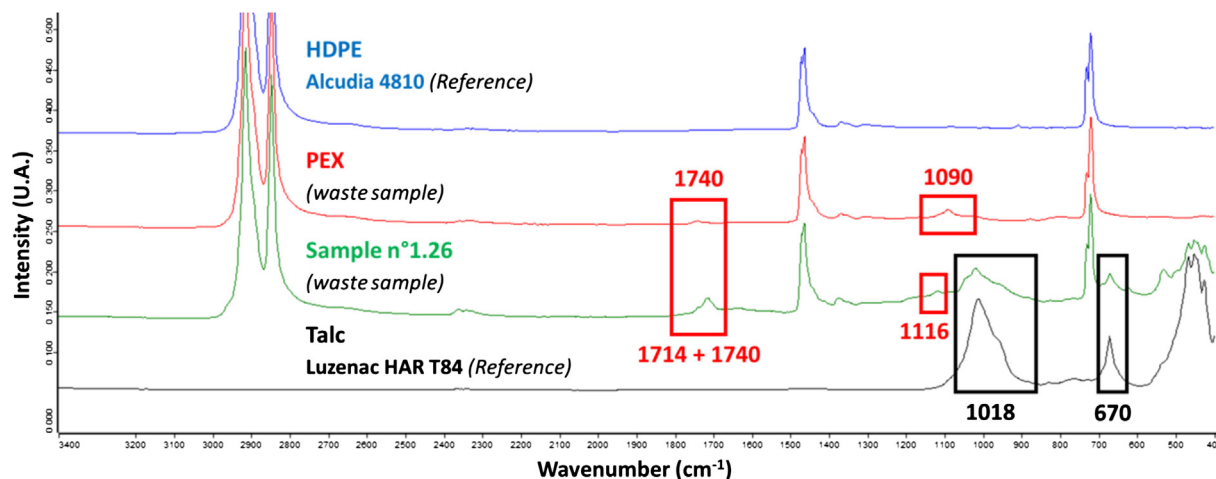


Fig. 3. Comparison in MIR of PEX sample to a waste sample of PE (n°1.26), the HDPE reference and a talc sample – polymer oxygenated groups marks framed in red, calcite peaks framed in black. (For interpretation of the references to color in this figure legend, the reader is referred to the web version of this article.)

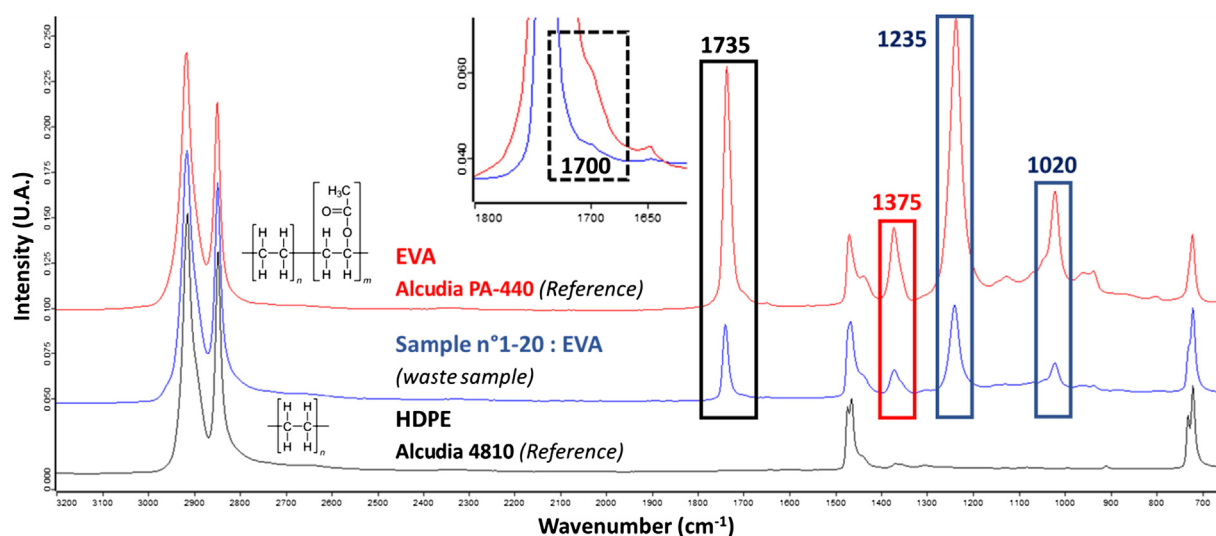


Fig. 4. EVA real waste sample comparison to HDPE and EVA reference samples in MIR – CH₃ framed in red, C–O framed in blue, C=O peak framed in black, C=O shoulder framed in dotted line in the magnification. (For interpretation of the references to color in this figure legend, the reader is referred to the web version of this article.)

information. EVA has simple peaks at 1460 and 720, and not double ones, because of its amorphous nature (Patel et al., 1998).

Waste samples spectra are similar to the reference sample, but with varying relative intensities. Ratios between peaks specific to ethylene (e.g. 720 or 1467) and vinyl acetate (e.g. 1735 for C=O stretching, or 1235 for C–O) hints the vinyl acetate fraction in this copolymer. In addition, EVA can be mixed with PE to have a tailored compromise between their properties (Patel et al., 1998; Takidis et al., 2003). If PE is added in great quantities, it could be expected to entail a display on the PE crystalline phase through duplication of the 1460 and 720 signals. Obviously, acetate signals will also relatively be weaker. However, differences between an EVA with low vinyl acetate content and a blend of EVA with PE seem difficult in MIR. A complete study with homemade samples at different ratios (at both copolymerization and blending states) could confirm/exclude this possibility. Thermal data, especially melting point(s), could remove any doubt.

It is surprising not to see CH and CH₃ group signals in the 2800–3000 range for EVA, especially when 1375 signal is clearly visible. Fig. 5 shows that the base of the two ethylene peaks is wider in EVA and could mask this signal. This can be linked to the shoulder

seen in the magnification of Fig. 4 at 1700 cm⁻¹ which can be associated with carboxylic acid whose O–H stretching manifests by large absorption bands centered on 2900, explaining this base widening. Indeed, acetic acid can be produced from EVA side reaction.

Industrial and laboratory MWIR discrimination of HDPE, LDPE, PEX and EVA seems strongly compromised as all spectra are almost identical, if not totally. LWIR could however easily identify EVA thanks to its very characteristic signals at 1375, 1235 and 1020 cm⁻¹. Outside MWIR or LWIR, the carbonyl peak at 1735 cm⁻¹ also allows fast identification. Complementary sorting technologies are advisable if tolerance thresholds are low (PEX and EVA should represent minorities as their applications are rather specific).

3.3. Propylene based polymers: PP homopolymer, PP copolymer and EPDM

Signals at 720 cm⁻¹ were found in numerous PP waste samples (12 on 16 samples identified as PP) whereas the reference sample, a polypropylene homopolymer (PPH), lacks it (Fig. 1). This proves

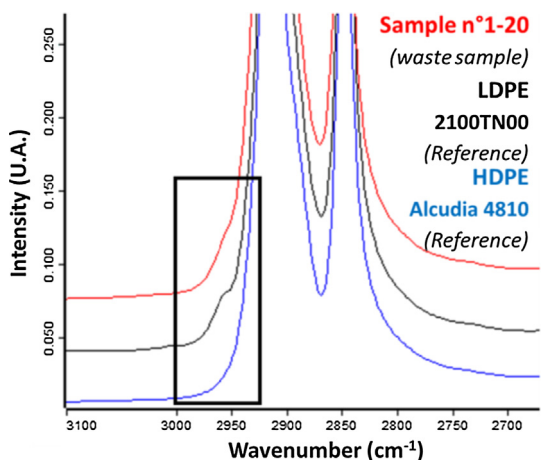


Fig. 5. CH₃ stretching peak position in HDPE, LDPE and EVA - black frame.

the presence of chaining CH₂, probably by copolymerization and/or blends involving ethylene. Thus, this peak is not specific of PE. However, it is as intense as other PPC signals on the LWIR range, as shown in the corresponding chart in [supporting information](#). Consequently, presence of this peak but absence of the others is specific of PE. Ethylene and propylene can also be copolymerized to form EPDM, also involving a diene monomer, often norbornene, to permit controlled crosslinking which gives it its elastomeric properties. EPDM is a terpolymer whereas EPR (ethylene-propylene rubber) can refer exclusively to the bipolymer ([Gensler et al., 2000](#)), even if the designation can be confusing. “PP copolymer”, “PPC”, “Hi-PP”, “co-PP” or “PP copo” is a class of PP with improved impact properties. However, it is not always clear if it addresses a random copolymer of propylene and ethylene, a block copolymer, a blend, or an EPDM/EPR added PP ([Bouvard et al., 2016](#); [Ramírez-Vargas et al., 2009](#); [Roumeli et al., 2014](#); [Zhou et al., 2008](#)). Similarly to the case of HDPE and LDPE, PPH has supe-

rior modulus and hardness but PPC is more processable and impact resistant.

LWIR spectra of [Fig. 6](#) show that EPDM and PPC are intermediate cases between HDPE and PPH, which can be considered as the extrema of the polyolefins range (UHMWPE is even more extreme but rather uncommon). The 720 peak(s) attest(s) for ethylene, and the 1375 mainly attests for propylene. The ≈ 1460 peak is a double sharp peak at $1460 + 1470 \text{ cm}^{-1}$ for chaining CH₂ as in PE but a single rounded band at ≈ 1455 for isolated CH₂ as in PPH ([Jung et al., 2018](#); [Noda et al., 2007](#)). The exact position on our PPC reference is at 1458, also detected on real samples whose 720 cm⁻¹ peak was relatively important, whereas this peak was at 1455 for others with relatively weak or absent (PPH) 720 signal. This intermediate position is surely the consequence of the convolution of ethylene and propylene units characteristic signals.

However, LWIR is limited at about 1350 cm⁻¹, below the red frame on [Fig. 6](#). Thus EPDM is very close to PE within this range and is another possible infusible impurity. Only the total amorphous nature of this material (as EVA) differentiates it from HDPE or even LDPE as this second one also displays duality in its 720 cm⁻¹ peak. The width of this possibly convoluted peak obtained through depreciated resolution could be a very sensible but potential differentiation element. Again, this 720 cm⁻¹ peak being at the lowest limit makes these considerations delicate. The same commentary can be made about PPH/PPC whose only distinction relies on this signal, as seen on [Fig. 6](#) and in the MWIR & LWIR charts in [supporting information](#).

MWIR spectra of [Fig. 7](#) also show the progressivity from HDPE to EPDM, to PP copo, to PP homo. As EPDM contains much more CH₃ than LDPE ([Fig. 2](#)), its $\approx 2950 \text{ cm}^{-1}$ shoulder is more strongly marked but still surely insufficient for discrimination with decreased sensitivity and resolution.

The PPC pattern is interesting by its relative heights. As the most right-handed peak becomes two, it highlights that CH₂ symmetric stretch ([Noda et al., 2007](#)) is at 2848 for PE, whereas it is lightly below, at 2839, for PP. [Fig. 7](#) also brings out the shoulder of the 2867 CH₃ symmetric stretch of PP found in both homo and

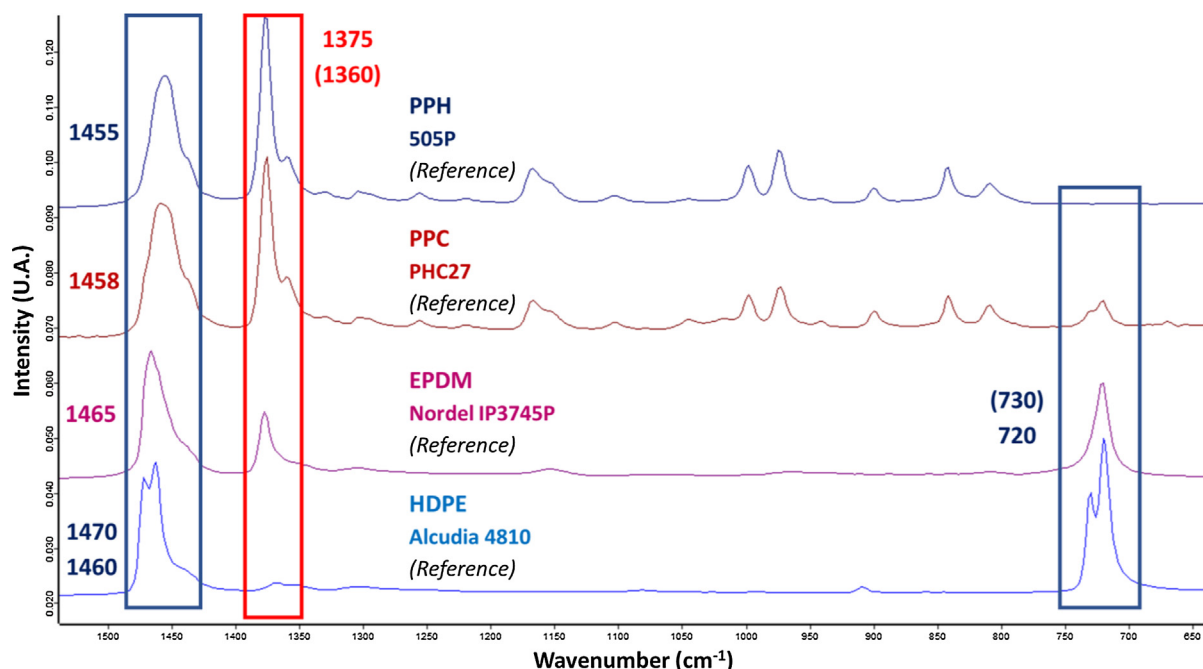


Fig. 6. Intermediate cases between 100w% ethylene and 100w% propylene in LWIR – CH₃ peak framed in red, CH₂ framed in blue. (For interpretation of the references to color in this figure legend, the reader is referred to the web version of this article.)

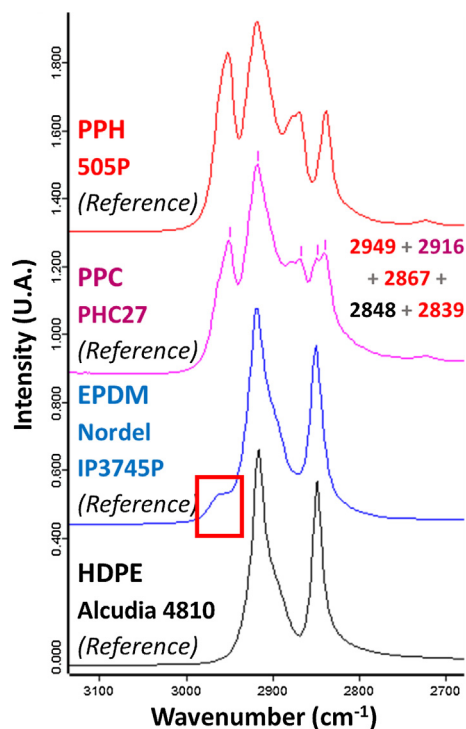


Fig. 7. HDPE, EPDM, PPC & PPH in MWIR – wavenumbers in red when specific to PP, in black for PE, purple for both – EPDM propylene peak framed. (For interpretation of the references to color in this figure legend, the reader is referred to the web version of this article.)

copolymer. Finally, the 2916 cm^{-1} peak is relatively stronger, especially against the 2950 cm^{-1} one, thanks to the ethylene participation. Waste samples showed that this relative intensity could hint homo/copo distinction but the absence/presence of the 720 cm^{-1} peak is much more reliable. Also, direct correlation of these respective signals intensities was not conclusive.

It appears that distinction between EPDM and PE, especially LDPE, can be delicate, as its differences rely on CH_3 content (no vinylic signal, as 1650 cm^{-1} was observed), expressed by a slight shoulder in MWIR and a peak out of the LWIR range as highlighted by the respective charts in [supporting information](#). No sample within the waste stock was identified as EPDM. Because of its crosslinked nature, it could be hazardous during recycling of mixed materials by being infusible.

For PP, two types, PPH and PPCn can be differentiated thanks to a peak at 720 cm^{-1} indicating chained CH_2 . A more specialized but laborious work could be done with DSC to further study and quantify the real nature of “PP copo” as real blends of PP and EPR/EPDM and not copolymers of ethylene or propylene themselves, or blends of it.

Even if “subtle” differentiations, between PEX/EVA/LDPE/HDPE/EPDM or PPH/PPC in MWIR and strict LWIR (especially without lowest wavenumbers), are difficult at laboratory scale and probably impossible in industrial conditions, one could still easily classify in “mainly polyethylene”, “mainly polypropylene” or “intermediate” classes through the number of signals and the relative intensities of specific signals as 720 cm^{-1} (polyethylene) or 1375 cm^{-1} (CH_3). In MWIR, shoulders can be seen appearing both sides of the twin peaks of PE for a low weight, an EVA or an EPDM and the central 2915 cm^{-1} of PP is notably stronger in PPC even if these differences are subtle and not as reliable as LWIR indicators mentioned above.

Every sample of the waste stock was identified thanks to the described methodology and supplementary standard samples of the Materiautech (Allizé-Plasturgie, n.d.) if necessary. This proves that every sample delivered spectra clear enough to permit identi-

fication. However, it must be considered that the studied waste stock is relatively limited in volume and origins to make present considerations universal. Though, it permitted to confirm findings obtained from standard samples.

3.4. Other considered polymers

3.4.1. PVC: Polyvinyl chloride

PVC is one of the oldest of currently widespread commercial polymers. It is principally found in building waste but can also be used to various other applications, with a minor fraction WEEE, and more largely in municipal waste deposits (Ciacci et al., 2016; Yu et al., 2016). It is important to keep PVC impurities at minimum when recycling other polymers due to its relative low decomposition temperature with release of hydrogen chloride which can promote other polymers degradation (Sadat-Shojai and Bakhshandeh, 2011; Yu et al., 2016). Moreover, it could entail damage to processing equipment through corrosion phenomena.

The particularity of PVC is its abundant C–Cl bonds whose stretching vibrations are associated with a group of strong signals framed in red on Fig. 8, roughly from 580 to 750 cm^{-1} , with two peaks culminating at 610 and 700 cm^{-1} , sadly currently out of the LWIR range. These bands can be depicted as the assembly of different C–Cl bonds, depending of their tacticity and crystallinity (Noda et al., 2007). The two main signals in LWIR are at 1245 and 965 cm^{-1} , which is a distinctive pattern, as highlighted by Table 3 or in [supporting information](#) as they are in empty columns. Their identification should not be problematic.

Fig. 9 shows that in MWIR, PVC looks like an intermediate case between HDPE and PP homo, with two strong peaks at 2912 and 2850 and a flat shoulder at $\approx 2965\text{ cm}^{-1}$ (Noda et al., 2007), more marked and above the 2950 shoulder of LDPE (Fig. 2) or EPDM (Fig. 7). Insufficient resolution and sensitivity could probably lead to confusion of PVC to PE or PP.

All of 15 analyzed PVC waste samples contain important amounts of calcite (CaCO_3), as it can be seen on spectra thanks to a very sharp signal at 875 cm^{-1} and a very specific triangular shape of the very intense and large signal at 1400 cm^{-1} (blue frames of Fig. 8). The signal at 2510 could even be seen in the MWIR range on Fig. 9, even if very weak.

Another frequently encountered signal is at 1730 cm^{-1} (black frame of Fig. 8), characteristic of C=O stretching, which could hint the presence of additives, especially phthalate plasticizers (Jimenez et al., 2001) or esters used as heat stabilizers, very frequently used in PVC (Yu et al., 2016).

LWIR distinction seems feasible (especially if ranges are extended towards lower wavenumbers) as numerous signals are observed along the range, the most two specific ones being at $610 + 700\text{ cm}^{-1}$. Conversely, MWIR could lead to confusion, especially with PE as both display strong peaks around 2915 and 2850 cm^{-1} . Only a slight shoulder differentiate them. As chloride is a heavier element than carbon or hydrogen, PVC could also be sorted thanks to X-rays technologies. Its high density (Gent et al., 2009), especially with high loading rates, can help its segregation through sink-float methods.

3.4.2. POM: Polyoxymethylene

POM is a technical polymer with a very high modulus and strong chemical resistance (Aronson et al., 2017; Pielichowska, 2015). Acetals, another name for POMs, can be divided in two types, homopolymers and copolymers, where oxyethylene units are distributed along the chain through copolymerization to enhance chemical and thermal stability (Aronson et al., 2017; Pan et al., 2004). Several POM waste samples were found in our stock, especially for rather small technical pieces with high modulus, as gear or small grids, in accordance with the literature

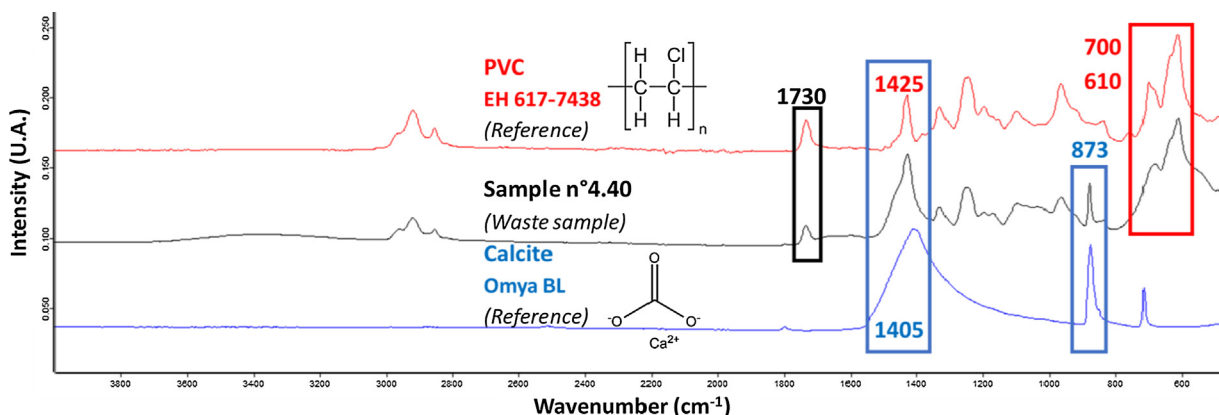


Fig. 8. MIR spectra of reference PVC, waste sample (n°4.40) and calcite reference – red frame for characteristic C–Cl peak, blue frames for calcite, black frame for additive. (For interpretation of the references to color in this figure legend, the reader is referred to the web version of this article.)

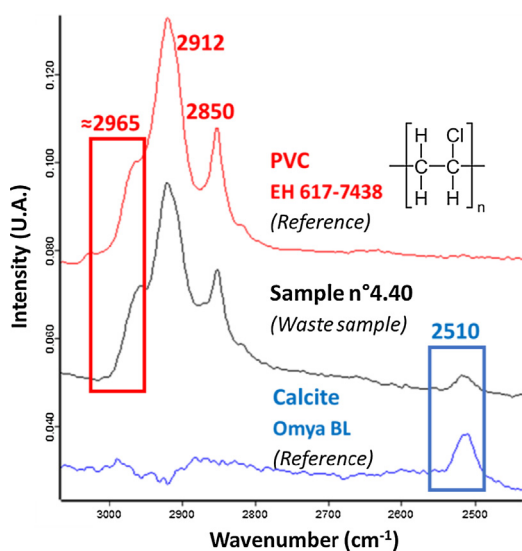


Fig. 9. MWIR spectra of reference PVC, waste sample (n°4.40) and calcite reference – 2965 shoulder of PVC framed in red, 2510 peak of calcite framed in blue. (For interpretation of the references to color in this figure legend, the reader is referred to the web version of this article.)

(Archodoulaki et al., 2007; Aronson et al., 2017). Even if their chemical pattern is visually close to polyolefins by its simplicity, compatibility seems severely compromised by polarity differences.

In the LWIR range, POM displays a very large signal from 1000 to 700 cm^{-1} with peaks at 890 and 925 cm^{-1} , framed in blue in Fig. 10. Its very specific shape is more reminiscent of minerals than organic materials. The sharp signals at 1087 and 630 cm^{-1} are also

characteristic, as no other or little materials display a peak there (empty column in the LWIR chart: Table 1 and supporting information), enabling easy identification.

In MWIR, POM pattern is reminiscent of PE but with a very specific signal at 2980, instead of 2950 cm^{-1} , as seen on Fig. 11 framed in red. This corresponds to an empty column in the supporting information chart. The 2790 cm^{-1} signal, framed in black on Fig. 11, is also characteristic, although very weak. Exact positions assessment is thus crucial for discrimination.

Spectra slightly differ in the MWIR range between waste samples and the reference, which could be due to differences of (co)polymerization or additives. A signal at 2855 cm^{-1} , framed in red on Fig. 11, could correspond to oxyethylene units as PEG (polyethylene glycol or POE, polyoxyethylene) displays a peak at 2860 cm^{-1} . Also, the 2980 cm^{-1} signal flattening seems linked to the occurrence of the 2855 cm^{-1} peak in the few presented examples and could be related to the 2945 cm^{-1} peak of PEG. As PVC, POM could also be sorted thanks to its high density (Gent et al., 2009) or X-rays technology because of its strong oxygen content.

PVC and POM display MWIR spectra strongly reminiscent of PE but the first one has a pronounced shoulder at 2965 cm^{-1} and the second one has its highest signal at 2980 instead of 2920 cm^{-1} for PE. Their LWIR spectra are exotic enough, especially POM, to enable easy identification. Indeed, it displays a rather large peak at 1087 and an even broader one at 890 cm^{-1} . Such large signals are unusual among polymers, enabling rapid identification.

3.5. Comparison between styrenics and polyolefins

Styrenics and polyolefins distinction is essential as they are not compatible (Perrin et al., 2016). Fig. 12 shows spectra of HDPE, PPH, HIPS and ABS on the whole MIR range at comparable intensity

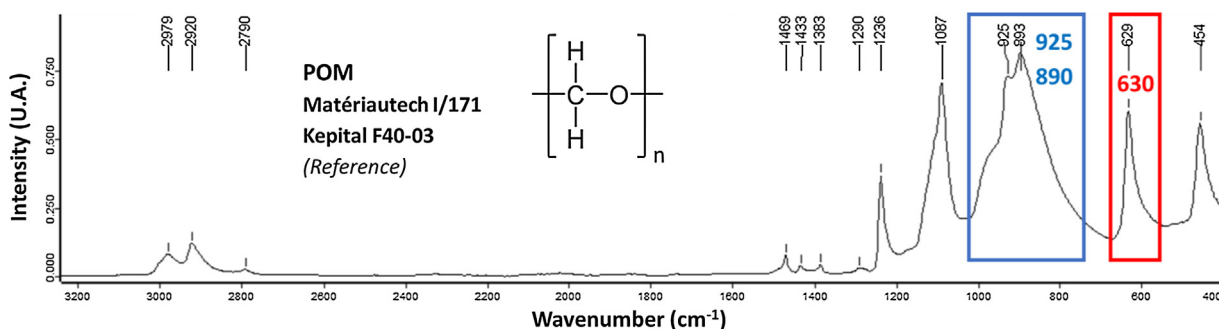


Fig. 10. POM reference sample MIR spectrum - characteristic peaks framed.

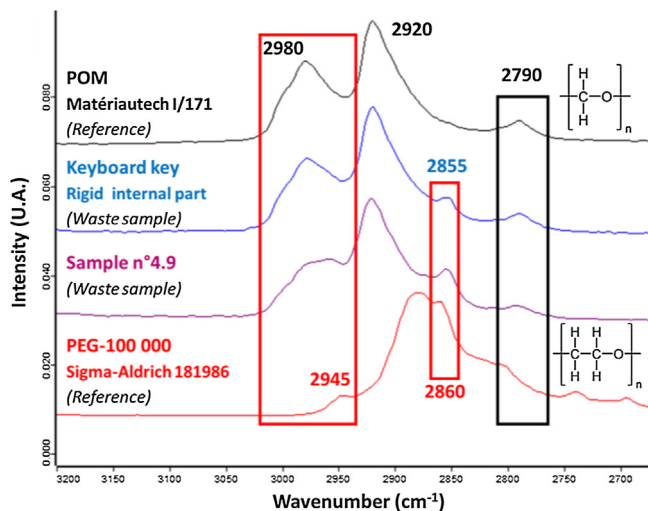


Fig. 11. Comparison of POM waste samples (keyboard key part and n°4.9) to POM and PEG references in MWIR – possible oxyethylene units peaks framed in red, specific 2790 POM signal. (For interpretation of the references to color in this figure legend, the reader is referred to the web version of this article.)

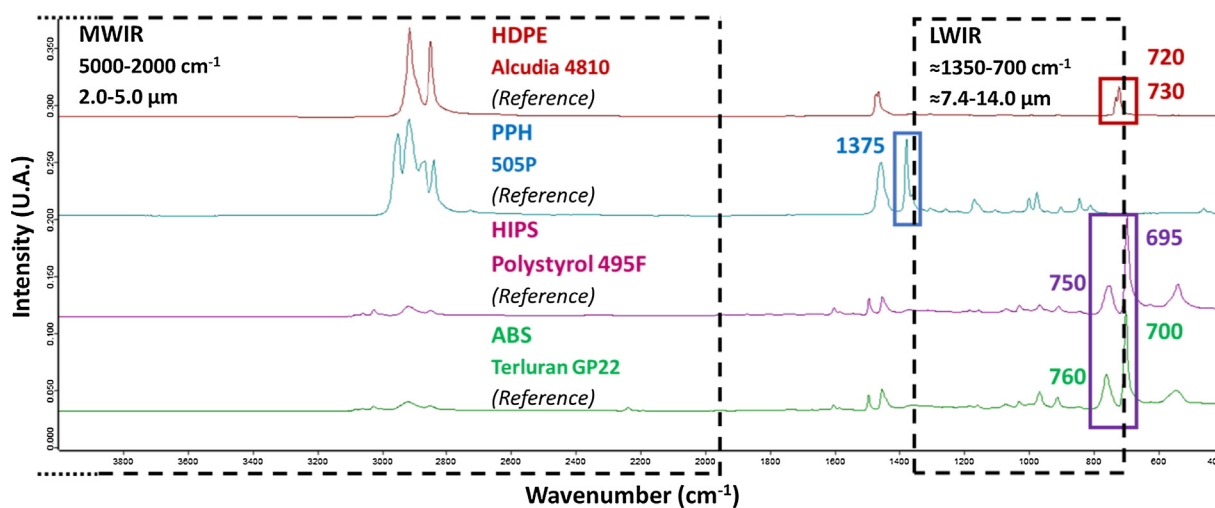


Fig. 12. MIR comparison of the main polyolefins and styrenics representative reference samples – dashed line frames for spectral ranges, brown frame for PE characteristic peak, blue frame for PP, purple frame for styrenics. (For interpretation of the references to color in this figure legend, the reader is referred to the web version of this article.)

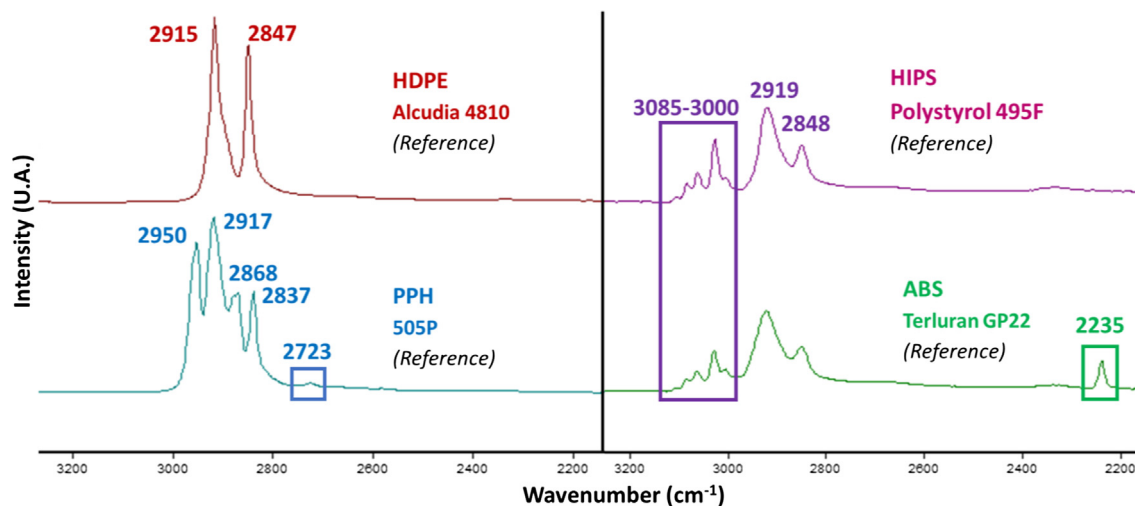


Fig. 13. MWIR comparison of the main polyolefins and styrenics representative reference samples – blue frame for PP, purple frame for styrenics, green frame for ABS. (For interpretation of the references to color in this figure legend, the reader is referred to the web version of this article.)

scales, by putting maximum peaks at same height. Polyolefins are more intense in MWIR, whereas styrenics are in LWIR. It must be noted that ATR mode gives stronger signals in LWIR than in MWIR, compared to transmission mode, because of the dependence of IR rays penetration to their wavelengths.

In LWIR, the most distinctive peaks are respectively 1375 cm^{-1} as the strongest for PP, $720 + 730\text{ cm}^{-1}$ as the strongest and almost alone for PE and $695 + 750/700 + 760\text{ cm}^{-1}$ for HIPS/ABS as discussed in a previous work (Signoret et al., 2019). These signals, as the $700\text{--}610\text{ cm}^{-1}$ peak of PVC, are near the limits of LWIR, if not beyond. Several rather weak signals scattered along the range for PP, HIPS and ABS could enable differentiation between styrenics and PP as their positions are different as proven in the LWIR chart in supporting information. The polybutadiene peaks at $910 + 965\text{ cm}^{-1}$ (just above the purple frame) are visibly stronger in the ABS reference but this difference is not reliable with real waste samples as they are subject to degradation. For polymer identification, one should prefer a camera with a range toward lowest wavenumbers (highest wavelengths) as signals are more critical and easily attainable there.

The MWIR range, way wider on the wavenumber scale but way shorter on the wavelength scale than LWIR, is poorer in signals,

and moreover distinctive signals, somehow simplifying considerations. The gap between the two domains also contains interesting signals, especially carbonyl peaks. Even if distinction seems possible nowadays, HSI cameras photosensors evolution toward larger acquisition ranges would be very beneficial to improve identification confidence.

Fig. 13 shows MWIR spectra of the four considered references, put at comparable intensity scales in the same way as above. Styrenics present aromatic C-H stretching from 3000 to 3085 cm^{-1} , an empty range for polyolefins, enabling discrimination if sensitivity is good enough as these peaks are weak. In addition, C-H stretching double peaks of styrenics are reminiscent of HDPE but slightly above, 2919 instead of 2915 cm^{-1} especially. Peak shapes are also sharper with PE. Industrial distinction within MWIR should be thus feasible.

In summary, styrenics can be rapidly differentiated in LWIR thanks to their specific signals at 750 + 695 cm^{-1} for HIPS and 760 + 700 for ABS corresponding to aromatic C-H bending. In LWIR, their aromatic C-H stretching above 3000 cm^{-1} characterize them. PE is characterized by its relative lack of signal but a specific peak at 720 cm^{-1} which can also be associated to PPC. PP has several weak signal along LWIR and a very specific signal at 2723 cm^{-1} in MWIR.

4. Conclusions

Polyolefins were considered in this study as they represent the most widespread polymer types, also very present in WEEE and ELV stocks, strongly concerned by black coloration that renders NIR-HSI ineffective, the most used technology in industrial acute sorting. Especially, they are strongly incompatible with styrenics, the first fraction of WEEE. MIR-HSI could participate in solving the problem of black plastic sorting and enable their proper valorization. As the acquisition parameters of MIR-HSI cameras are strongly limited compared with those of laboratory equipment, it is important to consider most of usable data. Thus, this study was dedicated to the scrutinization and discussion of polyolefins FTIR-ATR spectra.

In MIR, polyolefins are characterized by a low number of peaks, especially PE, because of their simple chemical natures, compared to other polymers. In MWIR, PE has only two clearly separated signals whereas PP has four close ones on a slightly wider range. In LWIR, PP has numerous weak signals and two very specific signals whereas PE has only one. However, among our references and waste samples, we found numerous intermediate cases between HDPE and PPH that can be considered the extrema of the polyolefins range. These samples combine both signals at different ratios. Specific distinction is challenging, even at laboratory scale, coercing to adopt more generalized classes, as “mainly ethylene” or “mainly propylene”. Also, both EVA and PEX are identical to PE in MWIR. LWIR can differentiate EVA from PE, but not PEX. PVC and POM display MWIR spectra strongly reminiscent of PE but with rounder shapes at slightly different wavenumbers. Their LWIR spectra are exotic enough, especially POM, to enable easy identification.

Comparisons between reference and real waste samples helped consolidating and giving nuances to the whole scheme. Generally, it has been found that polyolefins and styrenics distinction is easy to realize at laboratory scale and probably will not be a problem in industrial conditions. Polymer compatibility limits and post-sorting obtainable purities are to be closely considered to establish a pertinent recycling process. Future studies focusing on the impacts of acquisition parameters, plastic formulation (especially carbon black) and polymer ageing on spectra could help linking reference samples to real waste, but also to anticipate how they

could disrupt industrial acquisition and thus plastic sorting toward their valorization. Transpositions of presented considerations to an industrial tool (MIR-HSI), with degraded acquisition, in conjunction with the development of advanced classification algorithms will be the subject of another series of work.

Funding

This work was supported by BPI France via the FUI 20 (Fonds unique interministériel) grant.

Acknowledgements

The authors would like to thank Benjamin Gallard and Robert Lorquet for technical support, respectively for polymer processing and spectroscopy experiments. Suez Company is gratefully acknowledged for partnership in this work. Finally, the authors are very thankful to Allizé-Plasturgie for providing the numerous references of the Matériautech used in this work.

Appendix A. Supplementary material

Supplementary data to this article can be found online at <https://doi.org/10.1016/j.wasman.2019.08.010>.

References

- Aldrian, A., Ledersteger, A., Pomberger, R., 2015. Monitoring of WEEE plastics in regards to brominated flame retardants using handheld XRF. *Waste Manage.* 36, 297–304. <https://doi.org/10.1016/j.wasman.2014.10.025>.
- Allizé-Plasturgie, n.d. Allizé-Plasturgie : a professional organisation at the service of plastics and composites [Allizé-Plasturgie [WWW Document]. URL <https://www.allize-plasturgie.org/allize-plasturgie-professional-organisation-service-plastics-and-composites> (accessed 12.3.18).
- Archodoulaki, V.-M., Lüftl, S., Koch, T., Seidler, S., 2007. Property changes in polyoxymethylene (POM) resulting from processing, ageing and recycling. *Polym. Degrad. Stab.* 92, 2181–2189. <https://doi.org/10.1016/j.polymdegradstab.2007.02.024>.
- Aronson, A., Tartakovsky, K., Falkovich, R., Rabaev, M., Gottlieb, M., Kozlovsky, A., Levi, O., 2017. Failure analysis of aging in polyoxymethylene fuel valves using fractography and thermal-FTIR analysis. *Eng. Fail. Anal.* 79, 988–998. <https://doi.org/10.1016/j.engfailanal.2017.06.038>.
- Asadi, S., Babaizadeh, H., Foster, N., Broun, R., 2016. Environmental and economic life cycle assessment of PEX and copper plumbing systems: a case study. *J. Clean. Prod.* 137, 1228–1236. <https://doi.org/10.1016/j.jclepro.2016.08.006>.
- Baek, B.K., La, Y.H., Lee, A.S., Han, H., Kim, S.H., Hong, S.M., Koo, C.M., 2016. Decrosslinking reaction kinetics of silane-crosslinked polyethylene in sub- and supercritical fluids. *Polym. Degrad. Stab.* 130, 103–108. <https://doi.org/10.1016/j.polymdegradstab.2016.05.025>.
- Becker, W., Sachsenheimer, K., Klemenz, M., 2017. Detection of black plastics in the middle infrared spectrum (MIR) using photon up-conversion technique for polymer recycling purposes. *Polymers (Basel)* 9, 435. <https://doi.org/10.3390/polym9090435>.
- Beigbeder, J., Perrin, D., Mascaro, J.-F., Lopez-Cuesta, J.-M., 2013. Study of the physico-chemical properties of recycled polymers from waste electrical and electronic equipment (WEEE) sorted by high resolution near infrared devices. *Resour. Conserv. Recycl.* 78, 105–114. <https://doi.org/10.1016/j.resconrec.2013.07.006>.
- Bouvard, J.L., Denton, B., Freire, L., Horstemeyer, M.F., 2016. Modeling the mechanical behavior and impact properties of polypropylene and copolymer polypropylene. *J. Polym. Res.* 23, 70. <https://doi.org/10.1007/s10965-016-0947-z>.
- Celina, M.C., 2013. Review of polymer oxidation and its relationship with materials performance and lifetime prediction. *Polym. Degrad. Stab.* 98, 2419–2429. <https://doi.org/10.1016/j.polymdegradstab.2013.06.024>.
- Ciacchi, L., Passarini, F., Vassura, I., 2016. The European PVC cycle: In-use stock and flows. *Resour. Conserv. Recycl.* 123, 108–116. <https://doi.org/10.1016/j.resconrec.2016.08.008>.
- Cosate de Andrade, M.F., Souza, P.M.S., Cavalett, O., Morales, A.R., 2016. Life cycle assessment of poly(lactic acid) (PLA): comparison between chemical recycling, mechanical recycling and composting. *J. Polym. Environ.* 24, 372–384. <https://doi.org/10.1007/s10924-016-0787-2>.
- Cucchiella, F., D'Adamo, I., Lenny Koh, S.C., Rosa, P., 2015. Recycling of WEEEs: an economic assessment of present and future e-waste streams. *Renew. Sustain. Energy Rev.* 51, 263–272. <https://doi.org/10.1016/j.rser.2015.06.010>.
- da Silva, D.J., Wiebeck, H., 2017. Using PLS, iPLS and siPLS linear regressions to determine the composition of LDPE/HDPE blends: A comparison between

- confocal Raman and ATR-FTIR spectroscopies. *Vib. Spectrosc.* 92, 259–266. <https://doi.org/10.1016/j.vibspec.2017.08.009>.
- Delmas, M., Rossignol, R., Rodriguez, J.B., Christol, P., 2017. Design of InAs/GaSb superlattice infrared barrier detectors. *Superlattices Microstruct.* 104, 402–414. <https://doi.org/10.1016/j.spmi.2017.03.001>.
- Dimitrakakis, E., Janz, A., Bilitewski, B., Gidarakas, E., 2009. Small WEEE: determining recyclables and hazardous substances in plastics. *J. Hazard. Mater.* 161, 913–919. <https://doi.org/10.1016/j.jhazmat.2008.04.054>.
- Eriksen, M.K., Astrup, T.F., 2019. Characterisation of source-separated, rigid plastic waste and evaluation of recycling initiatives: effects of product design and source-separation system. *Waste Manage* 87, 161–172. <https://doi.org/10.1016/j.wasman.2019.02.006>.
- Gallen, C., Banks, A., Brandsma, S., Baduel, C., Thai, P., Eaglesham, G., Heffernan, A., Leonards, P., Bainton, P., Mueller, J.F., 2014. Towards development of a rapid and effective non-destructive testing strategy to identify brominated flame retardants in the plastics of consumer products. *Sci. Total Environ.* 491–492, 255–265. <https://doi.org/10.1016/j.scitotenv.2014.01.074>.
- Gallo, F., Fossi, C., Weber, R., Santillo, D., Sousa, J., Ingram, I., Nadal, A., Romano, D., 2018. Marine litter plastics and microplastics and their toxic chemicals components: the need for urgent preventive measures. *Environ. Sci. Eur.* 30, 13. <https://doi.org/10.1186/s12302-018-0139-z>.
- Gensler, R., Plummer, C.J.G., Grein, C., Kausch, H.-H., 2000. Influence of the loading rate on the fracture resistance of isotactic polypropylene and impact modified isotactic polypropylene. *Polymer (Guildf)* 41, 3809–3819. [https://doi.org/10.1016/S0032-3861\(99\)00593-5](https://doi.org/10.1016/S0032-3861(99)00593-5).
- Gent, M.R., Menendez, M., Torano, J., Diego, I., 2009. Recycling of plastic waste by density separation: prospects for optimization. *Waste Manage. Res.* 27, 175–187. <https://doi.org/10.1177/0734242X08096950>.
- Gulmine, J.V., Janissek, P.R., Heise, H.M., Akcelrud, L., 2002. Polyethylene characterization by FTIR. *Polym. Test.* 21, 557–563. [https://doi.org/10.1016/S0142-9418\(01\)00124-6](https://doi.org/10.1016/S0142-9418(01)00124-6).
- Gundupalli, S.P., Hait, S., Thakur, A., 2017. A review on automated sorting of source-separated municipal solid waste for recycling. *Waste Manage.* 60, 56–74. <https://doi.org/10.1016/j.wasman.2016.09.015>.
- Hagemann, H., Snyder, R.G., Peacock, A.J., Mandelkern, L., 1989. Quantitative infrared methods for the measurement of crystallinity and its temperature dependence: polyethylene. *Macromolecules* 22, 3600–3606. <https://doi.org/10.1021/ma00199a017>.
- Huerta Lwanga, E., Mendoza Vega, J., Ku Quej, V., Chi, J.de.los.A., Sanchez del Cid, L., Chi, C., Escalona Segura, G., Gertsen, H., Salánki, T., van der Ploeg, M., Koelmans, A.A., Geissen, V., 2017. Field evidence for transfer of plastic debris along a terrestrial food chain. *Sci. Rep.* 7, 14071. <https://doi.org/10.1038/s41598-017-14588-2>.
- Jimenez, A., Lopez, J., Iannoni, A., Kenny, J.M., 2001. Formulation and mechanical characterization of PVC plastisols based on low-toxicity additives. *J. Appl. Polym. Sci.* 81, 1881–1890. <https://doi.org/10.1002/app.1621>.
- Jung, M.R., Horgen, F.D., Orski, S.V., Rodriguez, C.V., Beers, K.L., Balazs, G.H., Jones, T. T., Work, T.M., Brignac, K.C., Royer, S.J., Hyrenbach, K.D., Jensen, B.A., Lynch, J.M., 2018. Validation of ATR FT-IR to identify polymers of plastic marine debris, including those ingested by marine organisms. *Mar. Pollut. Bull.* 127, 704–716. <https://doi.org/10.1016/j.marpolbul.2017.12.061>.
- Kassouf, A., Maalouly, J., Rutledge, D.N., Chebib, H., Ducruet, V., 2014. Rapid discrimination of plastic packaging materials using MIR spectroscopy coupled with independent components analysis (ICA). *Waste Manage.* 34, 2131–2138. <https://doi.org/10.1016/j.wasman.2014.06.015>.
- Kelley, K.M., Stenson, A.C., Dey, R., Whelton, A.J., 2014. Release of drinking water contaminants and odor impacts caused by green building cross-linked polyethylene (PEX) plumbing systems. *Water Res.* 67, 19–32. <https://doi.org/10.1016/j.watres.2014.08.051>.
- Koelmans, A.A., Besseling, E., Shim, W.J., Kiessling, T., Gutow, L., Thiel, M., 2015. *Marine Anthropogenic Litter*. Springer International Publishing, Cham.
- Küter, A., Reible, S., Geibig, T., Nüßler, D., Pohl, N., 2018. THz imaging for recycling of black plastics. *tm – Tech. Mess.* 85, 191–201. <https://doi.org/10.1515/teme-2017-0062>.
- Le Magueresse-Battistoni, B., Multigner, L., Beausoleil, C., Rousselle, C., 2018. Effects of bisphenol A on metabolism and evidences of a mode of action mediated through endocrine disruption. *Mol. Cell. Endocrinol.* 475, 74–91. <https://doi.org/10.1016/j.mce.2018.02.009>.
- Lebreton, L., Slat, B., Ferrari, F., Sainte-Rose, B., Aitken, J., Marthouse, R., Hajbane, S., Cunsolo, S., Schwarz, A., Levivier, A., Noble, K., Debeljak, P., Maral, H., Schoeneich-Argent, R., Brambini, R., Reisser, J., 2018. Evidence that the Great Pacific Garbage Patch is rapidly accumulating plastic. *Sci. Rep.* 8, 4666. <https://doi.org/10.1038/s41598-018-22939-w>.
- Li, W.C., Tse, H.F., Fok, L., 2016. Plastic waste in the marine environment: A review of sources, occurrence and effects. *Sci. Total Environ.* 566–567, 333–349. <https://doi.org/10.1016/j.scitotenv.2016.05.084>.
- Lingaih, N., Uddin, M.A., Muto, A., Imai, T., Sakata, Y., 2001. Removal of organic chlorine compounds by catalytic dehydrochlorination for the refinement of municipal waste plastic derived oil. *Fuel* 80, 1901–1905. [https://doi.org/10.1016/S0016-2361\(01\)00046-1](https://doi.org/10.1016/S0016-2361(01)00046-1).
- Maris, E., Botané, P., Wavrer, P., Froelich, D., 2015. Characterizing plastics originating from WEEE: a case study in France. *Miner. Eng.* 76, 28–37. <https://doi.org/10.1016/j.mineng.2014.12.034>.
- Matiddi, M., Hochscheid, S., Camedda, A., Bainsi, M., Cocumelli, C., Serena, F., Tomassetti, P., Travaglini, A., Marra, S., Campani, T., Scholl, F., Mancusi, C., Amato, E., Briguglio, P., Maffucci, F., Fossi, M.C., Bentivegna, F., de Lucia, G.A., 2017. Loggerhead sea turtles (*Caretta caretta*): a target species for monitoring litter ingested by marine organisms in the Mediterranean Sea. *Environ. Pollut.* 230, 199–209. <https://doi.org/10.1016/j.envpol.2017.06.054>.
- Muñoz, I., Colacino, J.A., Lewis, R.C., Arthur, A.E., Meeker, J.D., Ferguson, K.K., 2018. Associations between school lunch consumption and urinary phthalate metabolite concentrations in US children and adolescents: Results from NHANES 2003–2014. *Environ. Int.* 121, 287–295. <https://doi.org/10.1016/j.envint.2018.09.009>.
- Noda, I., Dowrey, A.E., Haynes, J.L., Marcott, C., 2007. Group frequency assignments for major infrared bands observed in common synthetic polymers. In: *Physical Properties of Polymers Handbook*. Springer, New York, New York, NY, pp. 395–406.
- Oliveira, G.L., Costa, M.F., 2010. Optimization of process conditions, characterization and mechanical properties of silane crosslinked high-density polyethylene. *Mater. Sci. Eng. A* 527, 4593–4599. <https://doi.org/10.1016/j.msea.2010.03.102>.
- Pan, G., Li, H., Cao, Y., 2004. ¹H-NMR investigation of the thermooxidation degradation of poly(oxyethylene) copolymers. *J. Appl. Polym. Sci.* 93, 577–583. <https://doi.org/10.1002/app.20481>.
- Patel, R.M., Saavedra, P., Hinton, C., DeGroot, J., 1998. Comparison of EVA and polyolefin plastomer as blend components in various film applications. *J. Plast. Film Sheeting*. <https://doi.org/10.1177/875608799801400407>.
- Peeters, J.R., Vanegas, P., Kellens, K., Wang, F., Huisman, J., Dewulf, W., Duflou, J.R., 2015. Forecasting waste compositions: a case study on plastic waste of electronic display housings. *Waste Manage.* 46, 28–39. <https://doi.org/10.1016/j.wasman.2015.09.019>.
- Peeters, J.R., Vanegas, P., Tange, L., Van Houwelingen, J., Duflou, J.R., 2014. Closed loop recycling of plastics containing Flame Retardants. *Resour. Conserv. Recycl.* 84, 35–43. <https://doi.org/10.1016/j.resconrec.2013.12.006>.
- Perrin, D., Mantaux, O., Ienny, P., Léger, R., Dumon, M., Lopez-Cuesta, J.M., 2016. Influence of impurities on the performances of HIPS recycled from Waste Electric and Electronic Equipment (WEEE). *Waste Manage.* 56, 438–445. <https://doi.org/10.1016/j.wasman.2016.07.014>.
- Pielichowska, K., 2015. Thermooxidative degradation of polyoxymethylene homo- and copolymer nanocomposites with hydroxyapatite: Kinetic and thermoanalytical study. *Thermochim. Acta* 600, 7–19. <https://doi.org/10.1016/j.tca.2014.11.016>.
- Pivnenko, K., Eriksen, M.K., Martín-Fernández, J.A., Eriksson, E., Astrup, T.F., 2016. Recycling of plastic waste: Presence of phthalates in plastics from households and industry. *Waste Manage.* 54, 44–52. <https://doi.org/10.1016/j.wasman.2016.05.014>.
- Pongstabodee, S., Kunachitpimol, N., Damronglerd, S., 2008. Combination of three-stage sink–float method and selective flotation technique for separation of mixed post-consumer plastic waste. *Waste Manage.* 28, 475–483. <https://doi.org/10.1016/j.wasman.2007.03.005>.
- Rabello, M.S., White, J.R., 1997. The role of physical structure and morphology in the photodegradation behaviour of polypropylene. *Polym. Degrad. Stab.* 56, 55–73. [https://doi.org/10.1016/S0141-3910\(96\)00202-9](https://doi.org/10.1016/S0141-3910(96)00202-9).
- Rahmani, S., Pour Khalili, N., Khan, F., Hassani, S., Ghafour-Boroujerdi, E., Abdollahi, M., 2018. Bisphenol A: What lies beneath its induced diabetes and the epigenetic modulation? *Life Sci.* 214, 136–144. <https://doi.org/10.1016/j.lfs.2018.10.044>.
- Ramírez-Vargas, E., Margarita Huerta-Martínez, B., Javier Medellín-Rodríguez, F., Sánchez-Valdes, S., 2009. Effect of heterophasic or random PP copolymer on the compatibility mechanism between EVA and PP copolymers. *J. Appl. Polym. Sci.* 112, 2290–2297. <https://doi.org/10.1002/app.29827>.
- Roumeli, E., Markoulis, A., Chrissafis, K., Avgeropoulos, A., Bikiaris, D., 2014. Substantial enhancement of PP random copolymer's thermal stability due to the addition of MWCNTs and nanodiamonds: decomposition kinetics and mechanism study. *J. Anal. Appl. Pyrolysis* 106, 71–80. <https://doi.org/10.1016/j.jaap.2013.12.012>.
- Rozenstein, O., Puckrin, E., Adamowski, J., 2017. Development of a new approach based on midwave infrared spectroscopy for post-consumer black plastic waste sorting in the recycling industry. *Waste Manage.* 68, 38–44. <https://doi.org/10.1016/j.wasman.2017.07.023>.
- Sadat-Shojai, M., Bakhshandeh, G.-R., 2011. Recycling of PVC wastes. *Polym. Degrad. Stab.* 96, 404–415. <https://doi.org/10.1016/j.polydegradstab.2010.12.001>.
- Serincan, U., Arikian, B., Senel, O., 2018. Direct growth of type II InAs/GaSb superlattice MWIR photodetector on GaAs substrate. *Superlattices Microstruct.* 120, 15–21. <https://doi.org/10.1016/j.spmi.2018.05.020>.
- Serranti, S., Gargiulo, A., Bonifazi, G., 2011. Characterization of post-consumer polyolefin wastes by hyperspectral imaging for quality control in recycling processes. *Waste Manage.* 31, 2217–2227. <https://doi.org/10.1016/j.wasman.2011.06.007>.
- Shamsaei, M., Aghayan, I., Kazemi, K.A., 2017. Experimental investigation of using cross-linked polyethylene waste as aggregate in roller compacted concrete pavement. *J. Clean. Prod.* 165, 290–297. <https://doi.org/10.1016/j.jclepro.2017.07.109>.
- Signoret, C., Caro-Bretelle, A.-S., Lopez-Cuesta, J.-M., Ienny, P., Perrin, D., 2019. MIR spectral characterization of plastic to enable discrimination in an industrial recycling context: I. Specific case of styrenic polymers. *Waste Manage.* 95, 513–525. <https://doi.org/10.1016/j.wasman.2019.05.050>.
- Steg, L., Vlek, C., 2009. Encouraging pro-environmental behaviour: An integrative review and research agenda. *J. Environ. Psychol.* 29, 309–317. <https://doi.org/10.1016/j.jenvp.2008.10.004>.
- Stenvall, E., Tostar, S., Boldizar, A., Foreman, M.R.S., Möller, K., 2013. An analysis of the composition and metal contamination of plastics from waste electrical and

- electronic equipment (WEEE). *Waste Manage.* 33, 915–922. <https://doi.org/10.1016/j.wasman.2012.12.022>.
- Takidis, G., Bikiaris, D.N., Papageorgiou, G.Z., Achilias, D.S., Sideridou, I., 2003. Compatibility of low-density polyethylene/poly(ethylene-co-vinyl acetate) binary blends prepared by melt mixing. *J. Appl. Polym. Sci.* 90, 841–852. <https://doi.org/10.1002/app.12663>.
- Thanh Truc, N.T., Lee, C.-H., Lee, B.-K., Mallampati, S.R., 2017. Development of hydrophobicity and selective separation of hazardous chlorinated plastics by mild heat treatment after PAC coating and froth flotation. *J. Hazard. Mater.* 321, 193–202. <https://doi.org/10.1016/j.jhazmat.2016.09.014>.
- The new plastics economy: Rethinking the future of plastics [WWW Document], 2016. . Ellen MacArthur Found. URL <https://www.ellenmacarthurfoundation.org/publications/the-new-plastics-economy-rethinking-the-future-of-plastics-catalysing-action>
- Thompson, R.C., Moore, C.J., vom Saal, F.S., Swan, S.H., 2009. Plastics, the environment and human health: current consensus and future trends. *Philos. Trans. R. Soc. B Biol. Sci.* 364, 2153–2166. <https://doi.org/10.1098/rstb.2009.0053>.
- Ueno, R., Ishii, K., Suzuki, K., Honda, H., Funaki, H., 2015. Infrared multispectral imaging with silicon-based multiband pass filter and infrared focal plane array. In: 2015 9th International Conference on Sensing Technology (ICST). IEEE, pp. 211–214.
- Wang, C., Wang, H., Fu, J., Liu, Y., 2015. Flotation separation of waste plastics for recycling—A review. *Waste Manage.* 41, 28–38. <https://doi.org/10.1016/j.wasman.2015.03.027>.
- WRAP, 2008. LCA of Management Options for Mixed Waste Plastics, Waste resource action programme (WRAP).
- Xanthos, D., Walker, T.R., 2017. International policies to reduce plastic marine pollution from single-use plastics (plastic bags and microbeads): a review. *Mar. Pollut. Bull.* 118, 17–26. <https://doi.org/10.1016/j.marpolbul.2017.02.048>.
- Yu, J., Sun, L., Ma, C., Qiao, Y., Yao, H., 2016. Thermal degradation of PVC: a review. *Waste Manage.* 48, 300–314. <https://doi.org/10.1016/j.wasman.2015.11.041>.
- Zhou, S., Wang, Z., Gui, Z., Hu, Y., 2008. A study of the novel intumescent flame-retarded PP/EPDM copolymer blends. *J. Appl. Polym. Sci.* 110, 3804–3811. <https://doi.org/10.1002/app.27727>.